ARTICLE / INVESTIGACIÓN

Synthesis, Structural Characterisation and Biological Activity; New Metal Complexes Derived from Semicarbazone Ligand

Baraa Kasim Mohammed[1]* and Enaam Ismail Yousif[2]

DOI. 10.21931/RB/2023.08.02.14

1Department of Chemistry, College of Education for Pure Science (Ibn Al-Haitham), Iraq

enaamismail@yahoo.com; anaam.i.y@ihcoedu.uobaghdad.edu.iq

2 Department of Chemistry, College of Education for Pure Science (Ibn Al-Haitham), University of Baghdad, Adhamiyah, Baghdad, Iraq

*Corresponding authors: Email: dr.baraakasim3@gmail.com,

Abstract: The results of synthesizing a novel tridentate Schiff-base ligand and its metal complexes have been given. The ligand itself is described as being tridentate. The synthesis of the ligand has the following chemical formula: (E)-2-((2S)-4-(tert-butyl) -2-((S)-(phenylamino) (p-tolyl) methyl) cyclohexylidene) hydrazine -1-carboxamide was produced as a byproduct of the reaction between benzoic acid and benzoic acid between (((4-(tert-butyl)-2-((S)-(phenylamino)(p-to and (HL). The ligand was reacted with 1:1 (L:M) mole ratios of ions containing Mn(II), Co(II), Ni(II), Cu(II), Zn(II), and Cd(II), which resulted in the production of title complexes. In cases where it was necessary, physicochemical techniques were utilized to characterize both the ligand and the complexes. Examples include magnetic susceptibility and conductance measurements, microanalysis of elements, nuclear magnetic resonance (1H, 13C), mass spectrometry, Fourier transform infrared (FT-IR), electronic spectra, and more. The results of these studies demonstrated that the ions Mn (II), Co (II), Cu(II), Ni(II), Zn(II), and Cd(II) can be partitioned into four-coordinate and six-coordinate complexes, respectively. In addition, the TGA was used to investigate whether or not the ligand and specific complexes were thermally stable. Several different bacterial and fungus strains were utilized to examine the ligand and its complexes for potential antibacterial activity. According to the findings, the complexes are far more effective than the free ligand in combating a wider variety of species.

Key words: Structural study, Metal complexes, Mannich -β-amino carbonyl, Thermal stability, *Staphylococcus aureus* (G+).

Introduction

It is common knowledge that chemical molecules with an azomethine group, collectively called Schiff bases, are known to have biological action[1]. It is one of the most important bonds representing many coordination complexes by linking metal elements and specializing in transition metal[2]. It is the elemental imine compound prepared by a German scientist named Hugo in 1864. It synthesizes a condensation reaction between a ketone or an aldehyde with primary amines[1]. It is one of the most important bonds representing many coordination complexes by linking metal elements and specializing with transition metal[3]. Because of their great variety of pharmacological and biological properties, Schiff complexes of important metals constitute a significant basic research topic for creating safe and effective therapeutic materials for treating bacterial infections and cancers. For example, the fact that transition metal complexes of Schiff base ligands with "O" and "N" donor atoms have antibacterial, antifungal, and anti-inflammatory characteristics makes them particularly significant[4], an anticonvulsant[5,6], an analgesic[7], an anthelmintic[8], an antitubercular[9], and an antioxidant[10]. Not very long ago, we attended the installation of the base Schiff and its complexes[11-13]. The ligand was synthesized from the reaction of the Mannich precursor ((((4)(tributyl)-2-(((S))-(phenylamino)(p-tolyl)methyl) cyclohexane-1-one)) with Semicarbazone, then the prepared compounds were tested, because of its effectiveness against bacteria and fungal organisms. In this study, we used two types of mushrooms and four distinct types of bacteria (Escherichia coli, Pseudomonas aeruginosa, Staphylococcus aureus, and Bacillus subtitles) (Candida albicans, and Rhizosporium). These species are responsible for most fungal infections found in humans. It is a common component of the flora that lives on human skin, vaginal membranes, and in the intestines of individuals living in healthy communities. In immunocompromised persons, fungal overgrowth and severe cutaneous or systemic infections caused by Clostridium albicans and other Candida species can cause morbidity and mortality. These infections can occur on the skin or elsewhere in the body[14].

Materials and methods

Reactor design

After obtaining the reagents from a commercial organization, you should use them precisely in the same manner you did to get the best results. To provide a reference, 1H- and 13C-NMR spectra were acquired for the linker in DMSO-d6 using a Brucker instrument at a frequency of 300 MHz for 1H-NMR and 75 MHz for 13C-NMR. KBr discs were used in an FT-IR spectrometer of the FTIR-600 type to gather data in the 4000-400 cm^{-1} to acquire FT-IR spectra. Electrospray (+) mass spectrometry has been worked on with the Sciex Esi mass analyzer. When taking the melting

Citation: Mohammed B K, Ismail Yousif E. Synthesis, Structural Characterisation and Biological Activity; New Metal Complexes Derived from Semicarbazone Ligand. Revis Bionatura 2023;8 (2) 14. http://dx.doi.org/10.21931/RB/2023.08.02.14

Received: 2 January 2023 / **Accepted:** 19 April 2023 / **Published:** 15 June 2023

Publisher's Note: Bionatura stays neutral with regard to jurisdictional claims in published maps and institutional affiliations.

point measurements, the researcher utilized a Stewart thermoelectric instrument of type SMP40. Electronic spectra were collected in the 1000–200 nm range on a Shimadzu UV-160 by using a 1.0 cm quartz cell at a concentration of 10^{-3} mol L^{-1} of samples in DMSO solutions. The spectra were taken in the region of 1000–200 nm. The measurements were obtained from a specific place referred to as the range. Using a Eutech Instruments Cyber scan, the temperature was maintained at room temperature. 510 digital conductivity meter calculation was made to establish the molar conductance of the complexes. The measurements were carried out on solutions of the chemicals in DMSO that ranged from 10^{-3}-10^{-5} M in concentration. For the element analysis (CHNS), we used the analyzer (Eager 300 for EA1112), and for the assessment of the metal content, we used the atomic absorption spectrophotometer manufactured by Shimadzu (A A-680G). To determine the amount of chloride present in the complexes, we carried out a potentiometric titration using a 686-Titro Processor-665 Dosim A-Metrohm/Swiss instrument. We utilized an STA PT-1000 manufactured by the Linseis Company in Germany for the thermogravimetric analysis, including TGA and DSC measurements. A magnetic susceptibility balance was used on Johnson Matthey to determine magnetic moments at a temperature of 306 kelvin. The ligand and its metal complexes were tested for their biological efficacy using an agar-well diffusion method against four different types of bacteria (*Escherichia coli, Pseudomonas aeruginosa, Staphylococcus aureus*, and *Bacillus subtitles*), as well as two different types of fungi. The results showed that the ligand and its metal complexes effectively inhibited the growth of the bacteria (*Candida albicans* and *Rhizosporium*). A spotless metallic borer was utilized to make wells in the medium at regular intervals of at least 6 mm in depth. The test samples were dispensed into the wells at the appropriate concentration of 1 mg/mL in DMSO (100µ L). After the plates had been prepared, they were kept in an incubator at 37 °C for twenty-four hours. Measurements of the inhibition zone's diameter are used to figure out the amount of activity (mm). To determine whether or not chemicals are effective against pathogenic bacteria, the well diffusion method was performed in an aerobic setting. On Mueller-Hinton agar, all potentially dangerous bacteria were tested for their capacity to inhibit growth.

Synthesis

Preparation of precursor

The preparation of (((4-(tert-butyl)-2-((S)-(phenylamino) (p-tolyl) methyl)cyclohexan-1-one)) was achieved adopting metod reported in[15,16].

Synthesis of Schiff-base ligand (HL)

With Respect to a Compound of (4-(tert-butyl)-2-((S)-(phenylamino)(p-tolyl)methyl)cyclohexan-1-one) During the addition of hot EtOH (0.5g, 1.4mmol), which was done so while stirring, a solution of semicarbazide (0.159g, 1.4mmol) in 15ml of EtOH with 3 drops of glacial acetic acid was created. The reaction mixture was refluxed for a total of six hours, during which time a white crystal formed. This crystal was filtered out, washed with five milliliters of cold ethanol, and then air-dried. The quantity produced was 0.3g (51%), and the melting point was 226-228°C.

Methodology for Complex Synthesis in General

Combined 0.4 millimoles of semicarbazone ligand with 10 milliliters of ethyl alcohol in a solution and added it while stirring to reduce the pH to approximately 9. After that, ten milliliters of ethanol that had been combined with a salt mixture of metal chloride were progressively added while the mixture was stirred. After that, the mixture was allowed to stand for ten minutes. This procedure was carried out on multiple occasions. After stirring the reaction mixture for four hours, a colorful precipitate had already begun forming in the mixture. As shown in Scheme 1, after creating a solid, it was filtered, then washed in 15 ml of cold 100% ethanol, and then finally air-dried (1). The yields, colors, and melting points of the complexes, as well as information regarding the quantities of metal salts, are included in the provided material (Table 1).

Results and discussion

After the reaction of (4-(tert-butyl)-2-((S)-(phenylamino) (p-tolyl)methyl)cyclohexan-1-one with semicarbazide in a 1:1 molar ratio at reflux, Scheme), the ligand ((E)-2-((2S)-4-(tert-butyl) -2-((S)-(phenylamino) (p-tolyl)methyl) (1). The ligand reacted with metal chloride salts of Mn(II), Co(II), Ni(II), Cu(II), and Cd(II) at a mole ratio of 1:1 (L: M), which resulted in the formation of six and four coordinate monomeric complexes, respectively. The monomeric chemicals that are produced as a result exist as solids at room temperature and are soluble in both DMSO and DMF. We have concluded that the complexes are extremely complicated and engage in highly coordinated activity based on the physical and chemical characteristics of the complexes. The results of Table 2 demonstrate that the data agree with the model that has been proposed. The results obtained by conducting the complexes in DMSO solutions containing these substances have demonstrated that there are both neutral and non-neutral, bringing the total number of complexes to (16).

Metal ion	Weight of metal salt(g)	Weight of complex(g)	Yield (%)	Colour	m.p.°C
[Mn(HL)Cl_2.H_2O]	0.079	0.17	41.87	pale pink	**>300***
[Co(HL)Cl_2.H_2O]	0.096	0.19	46.45	Pink	**280**
[Ni(HL) Cl_2.H_2O]	0.095	0.20	48.89	Pale green crystals	**268**
[Cu(HL)Cl_2H_2O]	0.068	0.21	50.98	green	**>300***
[Zn(HL)Cl]Cl	0.054	0.25	58.68	Deep-brown	**275**
[Cd(HL)Cl]Cl	**0.080**	**0.26**	**56.39**	**Deep-brown**	**290**

Table 1. Calculating HL complicated metal salt concentrations, products' hues, and temperatures of melting.

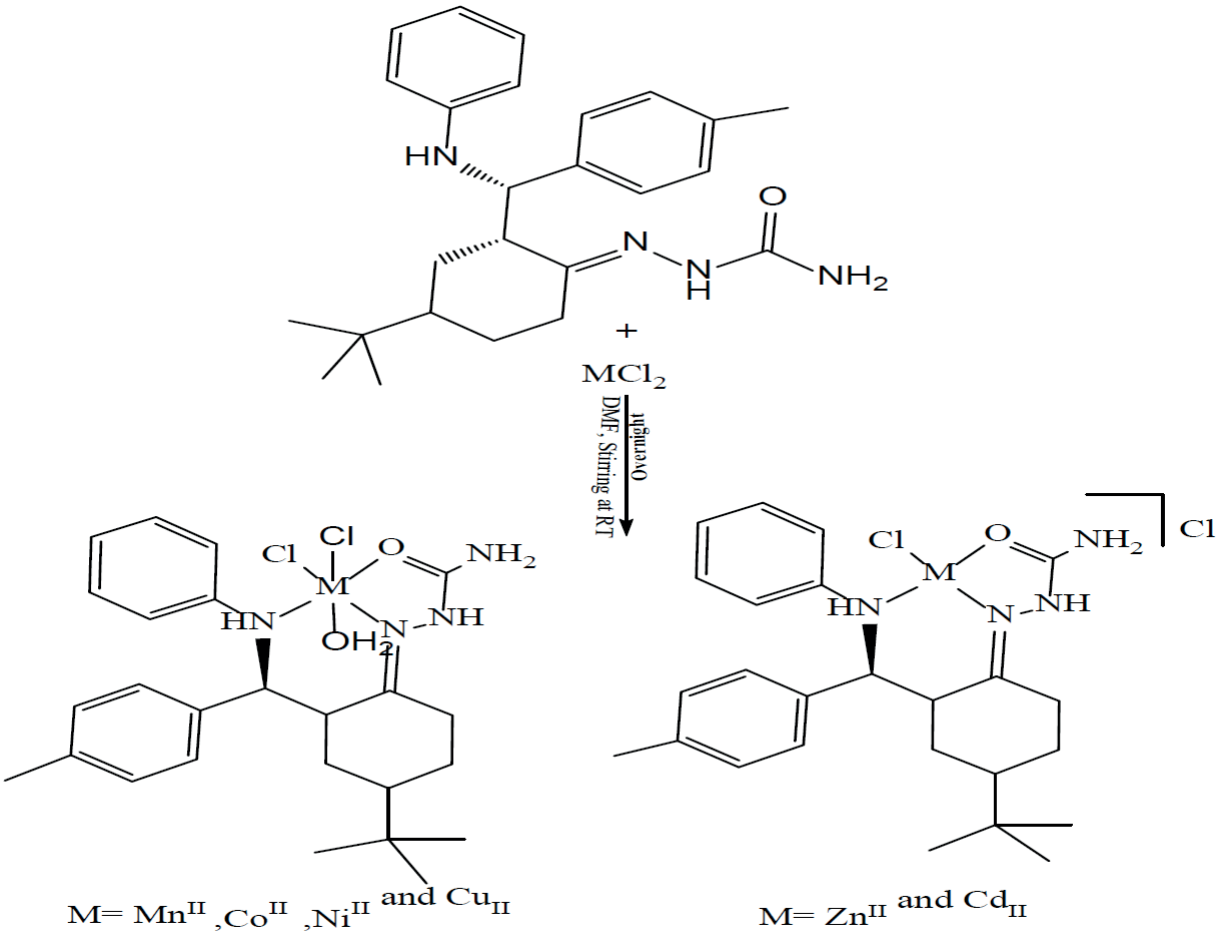

Figure 1. Synthesis route of HL complexes.

FT-IR Spectra

The FT-IR spectrum of the free semicarbazone ligand (HL) shows characteristic bands at 3460, 3282, 3194;3167,1693,1666and1600cm^{-1} that are attributed to v(NH)),v(NH)$_{am}$, v(NH$_2$)$_{sy,asy}$, v(C=O)$_{ket}$,v(C=N) imine and v(-C=C) aromatic, respectively[17,18]. The assigned complexes and their corresponding infrared data have been assembled in (Table 3). The creation of complexes was confirmed by analyzing their FT-IR spectra, which revealed altered ligand bands. The imine band, first detected at 1666 cm^{-1} in the free ligand (HL), was shown to have migrated to a lower frequency and be present at around 1600-1658 cm^{-1} in complexes[19]. This change demonstrated the iminic group's nitrogen atom was playing a role in the coordination process with the metal center[20,21]. This shift may indicate that the ligand is coordinated to the metal ions via the O atom when compared to the shift in the v(C-O) group in the spectra of complexes, which happened in comparison to the shift in the free ligand. Novel bands, identified as v (M-O), can be seen in the FT-IR spectra of the complexes between 609 and 694 cm^{-1} and 401-497 cm^{-1}, respectively (M-N). 22,23 Additionally, bands were seen in the 227-299 cm^{-1} range that was attributed to (M-Cl)[22].

NMR Spectra

NMR spectra of HL in dimethylsulfoxide-d6 displayed characteristic peaks at δH;(400MHz, DMSO-d6): 7.39-7.37 ($C_{14,14}$`)-H (1H, d, J = 17Hz). 7.23-7.22 ($C_{13,13}$`)-H (1H, t, J = 3Hz). 7.20-7.18 , 7.15 ($C_{15,15}$`)-H (1H, d, J = 12Hz) , ($C_{10,10}$`)-H (1H, d, J = 18Hz). 2.32-2.31 ($C_{9,9}$-)-H (1H, t, J =8Hz). 6.44 NHc (1H, N-H, d, J = 4Hz). 2.64-2.62 (C7-H) (1H, d). 2.46-2.44 (C_2)-H (1H, m, J=4Hz). 2.26:2.24 (C_6)-H (2H, t). 2.18 CH_3 C_{17}-H (3H, s,–(Me)). (C_5)-H (2H, m). 1.23. 1.06;1.04 C_3-H (2H, t). 1.00;0.99 C_4-H (1H, m). 0.71-0.57, 3(CH_3) C_{18}-H (9H, s).10.19-10.16 (NH_b). 8.19 NHa ,Fig.1. The 13C-NMR spectrum of the HL in dimethylsulfoxide-d6 showed peaks at;(100MHz, dimethylsulfoxide-d6): 147.6 ,137.5,135.6 (C_{12}), (C_8) and (C_{11}).($C_{14,14}$-), ($C_{10,10}$-),($C_{9,9}$-), (C_{15}), and ($C_{13,13}$-) were detected at 129.5,128.8, 126.5,120.8 and 113.5. 60.0, 41.6, 40.8,32.5, 32.81 ,32.17 (C_7) (C_4),(C_2) (C_{16}) (C_6) (C_5) . (C_{18}) (C_3), (C_{17}) 27.6,22.7 , 21.3. C=O δ = 179.0. (-C=N-) 166.60. 38.52-39 ppm, Fig.2.

Mass spectrum

The electrospray (+) mass spectrum of HL showed a band of at m/z = 405.60 amu (3%) (M-H)$^+$ calculated for $C_{25}H_{33}N_4O^+$ requires = 406.57. Peaks detected at m/z = 329.47(5 %), 272.35 (22 %), 218.28 (13 %), 117.17 (40 %), and 77.11 (29 %), related to [(M-H)-($C_2H_8N_2O$)], [(M-H)-($C_2H_8N_2O$) + (C_4H_9+)], [(M-H)-($C_2H_8N_2O$) + (C_4H_9+) + (C_3H_4N+)], [(M-H) ($C_2H_8N_2O$) + (C_4H_9+) + (C_3H_4N+) + (C_7H_3N.+)] and [(M-H)-($C_2H_8N_2O$)+(C_4H_9+) + (C_3H_4N+) + (C_7H_3N.+) +(C_3H_3.)], respectively, Fig.3.

Electronic Spectra and Magnetic Moment Measurements

Strong absorption peak may be seen in the UV-Vis spectrum of HL, (228nm =43859cm^{-1}, εmax= 458molar^{1} cm^{-1}), (284nm =35211cm^{-1}, εmax= 807 molar^{-1}cm^{-1}) and (347nm =28818cm^{-1}, εmax= 515 molar^{-1}cm^{-1}) which are assigned to

Complex	Molecular formula	M.Wt	Micro analysis found, calculated (%)				
			C	H	N	M	Cl
[Mn(HL)Cl$_2$H$_2$O]	$C_{25}H_{36}MnN_4O_2.Cl_2$	550.6	54.10 (54.40)	5.32 (6.53)	9.15 (10.17)	8.78 (9.97)	11.71 (12.89)
[Co(HL) Cl$_2$H$_2$O]	$C_{25}H_{36}CoN_4O_2.Cl_2$	554.6	53.11 (54.09)	6.21 (6.49)	9.11 (10.09)	10.24 (10.62)	11.02 (12.80)
[Ni(HL) Cl$_2$ H$_2$O]	$C_{25}H_{36}NiN_4O_2.Cl_2$	554.36	53.21 (54.11)	5.40 (6.49)	9.44 (10.10)	9.34 (10.58)	11.33 (12.80)
[Cu(HL) Cl$_2$H$_2$O]	$C_{25}H_{36}CuN_4O_2.Cl_2$	559.21	52.55 (53.64)	5.35 (6.43)	9.56 (10.01)	10.22 (11.36)	11.53 (12.69)
[Zn(HL) Cl]Cl	$C_{25}H_{34}ZnN_4O.Cl_2$	542.95	54.21 (55.25)	5.67 (6.26)	9.03 (10.31)	11.05 (12.04)	12.11 (13.07)
[Cd(HL) Cl]Cl	$C_{25}H_{34}CdN_4O.Cl_2$	589.98	49.44 (50.84)	4.35 (5.76)	8.55 (9.49)	18.21 (19.05)	11.11 (12.03)

Table 2. Characterization of HL and its compounds on a microscopic scale, together with their physical properties.

Compounds	ν(NH)	ν(NH) am	ν(NH2)sy,asy	ν(H2O)	ν(C=O)	ν(C=N)	δ(N-H)	ν(C=C)	ν(M-O)	ν(M-N)	ν(M-Cl)
HL	3460	3282	3194, 3167	-	1693	1666	1600	1504	-	-	-
[Mn(HL)Cl2H2O]	3431	3404	3342	3157	1668	1627	1595	1564	671,622	480,426	291,260
[Co(HL)Cl2H2O]	3440	3421	3301, 3240	3197	1678	1658	1593	1540	694,621	455,405	299,254
[Ni(HL) Cl2H2O]	3436	3394	3342, 3139	3114	1652	1631	1575	1527	632	457,422	283,266
[Cu(HL)Cl2H2O]	3525	3421	3363, 3255	3163	1678	1658	1593	1527	667,624	497,424	287,243
[Zn(HL)Cl] Cl	3437	3360	3278, 3197	-	1680	1600	1562	1504	624	447,401	281
[Cd(HL)Cl] Cl	3450	3286	3190, 3167	-	1681	1647	1597	1508	609	482,451	227

Table 3. Analysis of HL and its compounds using FT-IR spectroscopy (cm^{-1}).

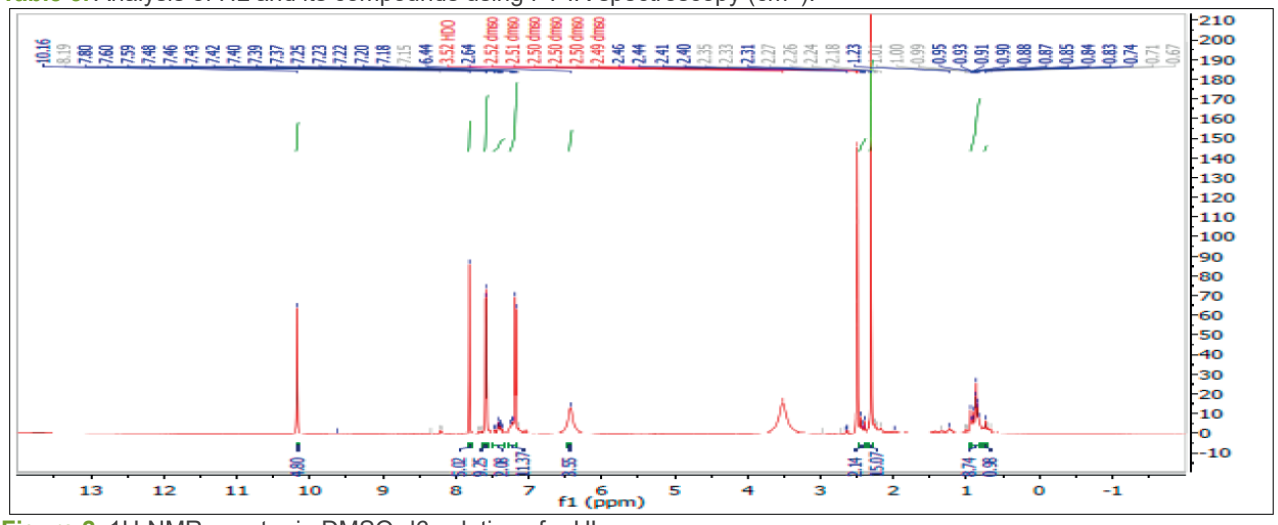

Figure 2. 1H-NMR spectra in DMSO-d6 solutions for HL.

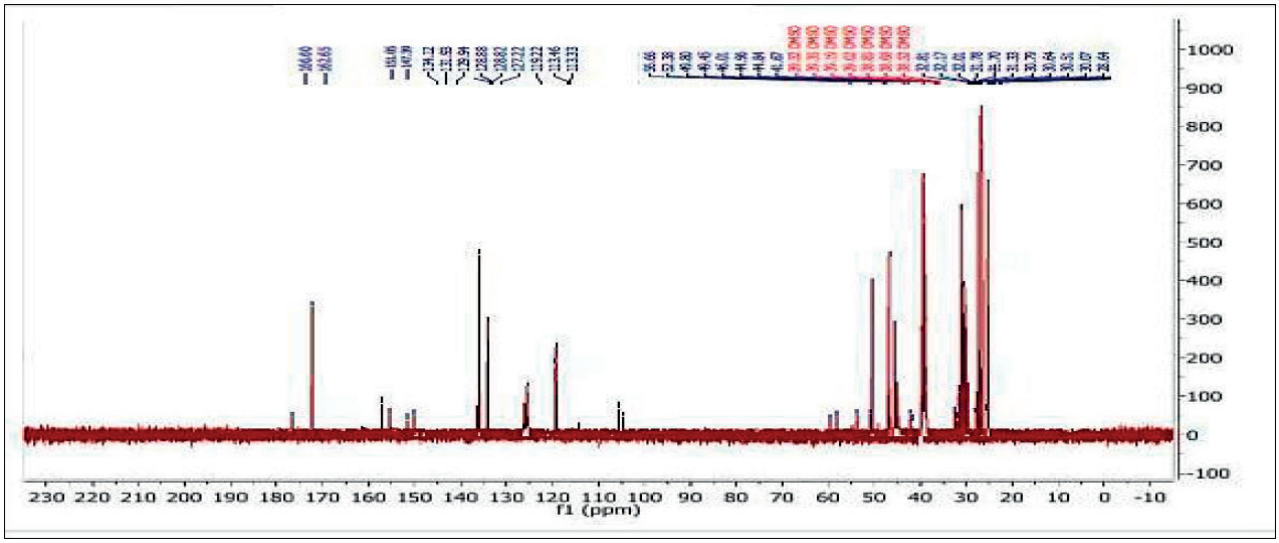

Figure 3. ^{13}C-NMR spectra in DMSO-d6 solutions for HL.

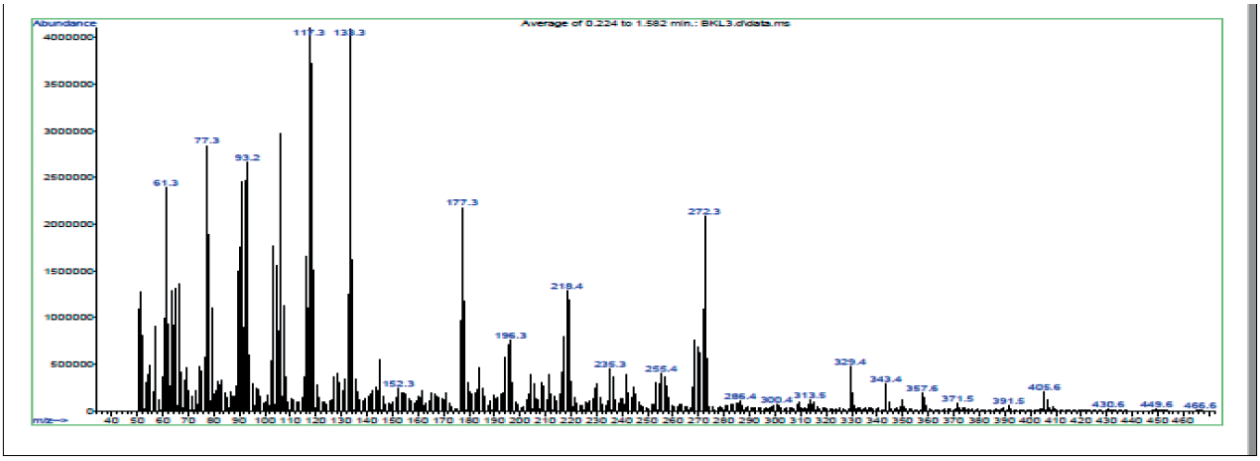

Figure 4. The electrospray (+) mass spectrum of HL.

π→π*, π→π*and n→π* transitions, respectively[23]. Electronic spectra and magnetic moment data for HL and its compounds are compiled in (Table 4). The electronic spectra of the complexes exhibit several peaks in the vicinity of 214-269 and 301-310 nm. These peaks can be attributed to π→π*, n→π* and charge transfer, respectively[24]. Peaks in the d-d region are observed at 841 nm in the electronic spectra of the Mn(I) complex, and these peaks are associated to $6A_1g \rightarrow 4T_1g(4G)$ transitions[23]. Because the Co(II) combination formed a distorted octahedral structure[23], the electronic spectrum of the compound conforms to its magnetic values. The electronic spectra of the Ni(II) complex displayed a peak in the d-d region at 794. This peak was caused by the type transition $3A_2g(F) \rightarrow 3T_2g(F)$, and it indicated that the geometry of Ni atom[24] was octahedral. In the d-d region, the Cu(II) complex produced one peak at 941 that was attributed to the $2Eg \rightarrow 2T_2g$ transition. This confirmed a distorted octahedral structure about the Cu atom[25]. This spectrum agrees with the eff value that was given for the geometry that was shown. In which the spectra of the Zn(II) and Cd(II) complexes had distinct bands for the → π* and n → π associative domain transitions, respectively. It has been suggested that the tetrahedral geometric structure of the center of Zn(II) and Cd(II) is present[26].

Thermal Analysis

The thermal decomposition of solid ligands (HL) was investigated in an atmosphere composed of nitrogen. After reaching 800 degrees Celsius, the sample experienced a weight drop that was measured. The results of the TGA analysis showed quite clearly that the breakdown of the ligand occurs in four distinct stages (Fig. 4). The weight loss at the 1st peak, as indicated by the TGA curve at 97-215 °C, many attributes to the loss of ($2NH_3$) segments and one acetylene molecule (obs. = 0.1701 mg, 8.418 % ; calc.= 0.1701 mg, 8.418 %). The second step happened from 215 to 359 °C stated the elimination of (C_5H_4+C-$(CH_3)_3$+NH_3+-CO+$N(CH_3)_2$+C_6H_6) fragments; (obs. = 1.439 mg, 71.19 % ; calc. = 1.439 mg, 71.19 %). The third step recorded at 359-532 °C may indicate the loss of the ($2CH_4$+$3H_2$) segment (obs. = 0.1913 mg, 9.466 %; calc. = 0.1913 mg, 9.466 %). The final step at 532-800 °C is attached to the (CH_3+$4H_2$) segment (obs. = 0.1211 mg, 5.991 %; calc. = 0.1211 mg, 5.991 %). The thermogram $[Co(HL)_2Cl_2H_2O]$ complex proceeds in four steps, Fig 5. The loss of one molecule of the H_2O segments may be responsible for the appearance of the first peak, which was observed between 49 and 132 degrees Celsius (obs. =0.083 mg, 3.271%; calc. =0.082 mg, 3.52%). The second step occurred at 132-194°C, indicating the loss of ($4H_2$+ CH_4) fragment; (obs.=0.2078mg, 5.033%;calc.=0.200mg, 5.011%). The third step recorded at 194-370°C indicated the loss of ($2NH_3$) fragment, (obs.=0.253mg,6.133%;calc.=0.230mg,6.1%). The ford step recorded at 370-800°C indicated the loss of (CO + Cl_2 + $2H_2$ + N_2H_4) fragment, (obs.=1.006mg, 24.38%; calc.=0.998mg, 24.30%). The final residue of the ($2CH_4$ + CH_3 + C_2H_6 + C_3H_6 + $2C_6H_6$ + $3H_2$ + Co) calc.= 340.69mg, 61.37%. The thermogram of $[Cu(HL)_2Cl_2H_2O]$ is depicted in, Fig 6. The first peak detected at 52-172°C may attribute to the loss of a molecule of the (H_2O + CH_3) segment; (obs.=0.1974mg, 6.058%; calc.= 0.1954mg, 6.016). The second step occurred at 172-235°C indicated the loss of (CO + Cl_2 + CH_4 + $2NH_3$) fragment; (obs.=0.87mg,26.70%; calc.=0.85mg,26.53%). The third peak detected at 235-642°C may attribute to the loss of a molecule of the (Cu + $2H_2$) segment; (obs.=0.391mg, 12.02%; calc.= 0.380mg, 11.86). The four peak detected at 642-800°C may attribute to the loss of a molecule of the (N_2H_4 + $4H_2$) segment; (obs.=0.2374mg, 7.285%; calc.= 0.2300mg, 7.186). The final residue of the ($C_{13}H_{19}$ + $2NH_3$ + Cu) calc.= 304.35mg, 48.31%. The burning of the organic ligand in an environment composed mostly of nitrogen.

Biological Activity

Tests were conducted on the semicarbazone (HL) ligand as well as its analogs against four distinct types of bacteria, including two Gram-negative bacteria and two Gram-positive bacteria (*Staphylococcus aureus, Bacillus stubtilis, Escherichia coli* and *Pseudomonas aeruginosa*). The Mueller-Hinton agar technique is utilized to analyze all 27 of the chemicals. The DMSO solvent did not affect whatsoever the compounds that were investigated. DMSO in a concentration of 100 ppm is used in the solution. Table 5 shows that the ligand (HL) had no effect whatsoever on any of the tested bacteria types. When it came to eliminating bacteria of every variety, the HL complexes proved to be more effective than the free ligand (HL). The formation of complexes results in an enhancement of the antibacterial effect. This phenomenon and the chelation hypothesis of why complexes become more active might be related to one another in some way. Therefore, chelation reduces the polarity of the metal atom, which results in some of the atom's positive charge being shared with the donor group and possibly in the delocalization of electrons across the entirety of

Complex	λ_{nm}	Wave number $\bar{\upsilon}$ (cm^{-1})	Molar extinction coefficient ε_{max} ($dm^3\ mol^{-1}\ cm^{-1}$)	Assignment	Suggested geometry	μeff
[Mn (HL)Cl_2 H_2O]	298 385 841	33557 25974 11890	2296 1323 66	Intra-ligand π → π*,n→π* CT $^6A_1g \rightarrow {}^4T_1g(^4G)$	Distorted octahedral	6.06
[Co(HL) Cl_2 H_2O]	267 301 681 934	37453 33222 14684 10706	1400 1320 87 7	Intra-ligand π → π*,n→π* CT $^4T_1g^{(F)} \rightarrow {}^4A_2g^{(F)}$ $^4T_1g^{(F)} \rightarrow {}^4T_2g^{(p)}$	Distorted octahedral	5.19
[Ni(HL) Cl_2 H_2O]	285 350 421 794	26954 28571 23753 12594	2323 392 45 18	Intra-ligand π → π*,n→π* CT $^3A_2g^{(F)} \rightarrow {}^3T_1g^{(P)}$ $^3A_2g^{(F)} \rightarrow {}^3T_2g^{(F)}$	Distorted octahedral	3.10
[Cu(HL)Cl_2H_2O]	293 348 941	34129 28735 10626	2186 2498 42	Intra-ligand π → π*,n→π* CT $^2Eg \rightarrow {}^2T_2g$	Distorted octahedral	1.89
[Zn(HL) Cl]Cl	270 298	27037 33557	1768 1884	Intra-ligand π → π*,n→π* CT	Tetrahedral	Diamagnetic
[Cd(HL)Cl]Cl	268 301	37313 33222	1554 1384	Intra-ligand π → π*,n→π* CT	Tetrahedral	Diamagnetic

Table 4. Data on electronic spectra in solutions of DMSO, as well as magnetic moments of HL complexes.

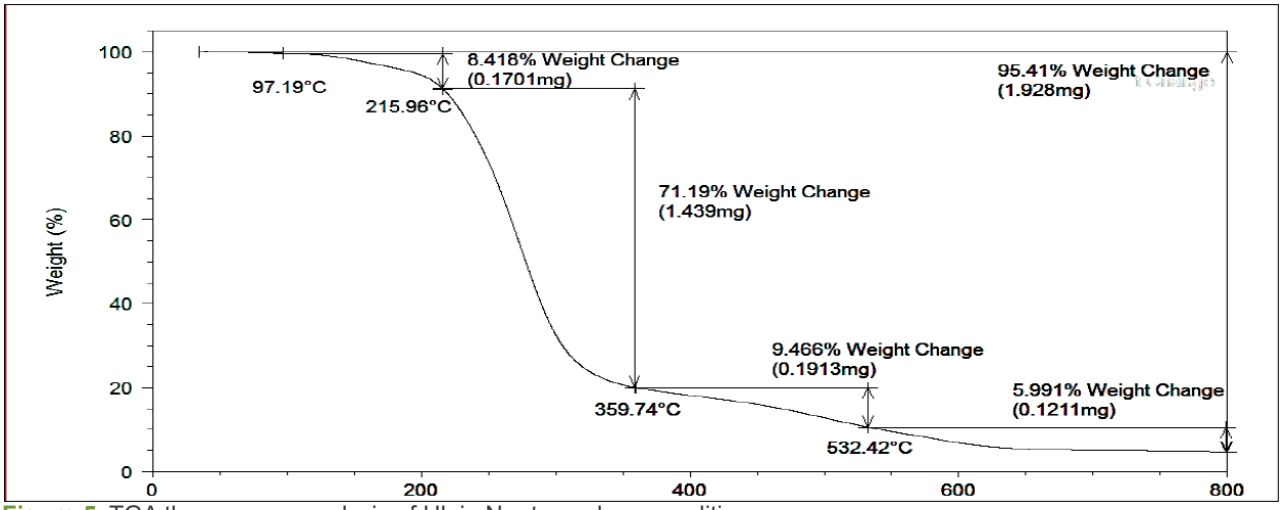

Figure 5. TGA thermogram analysis of HL in N_2 atmosphere conditions.

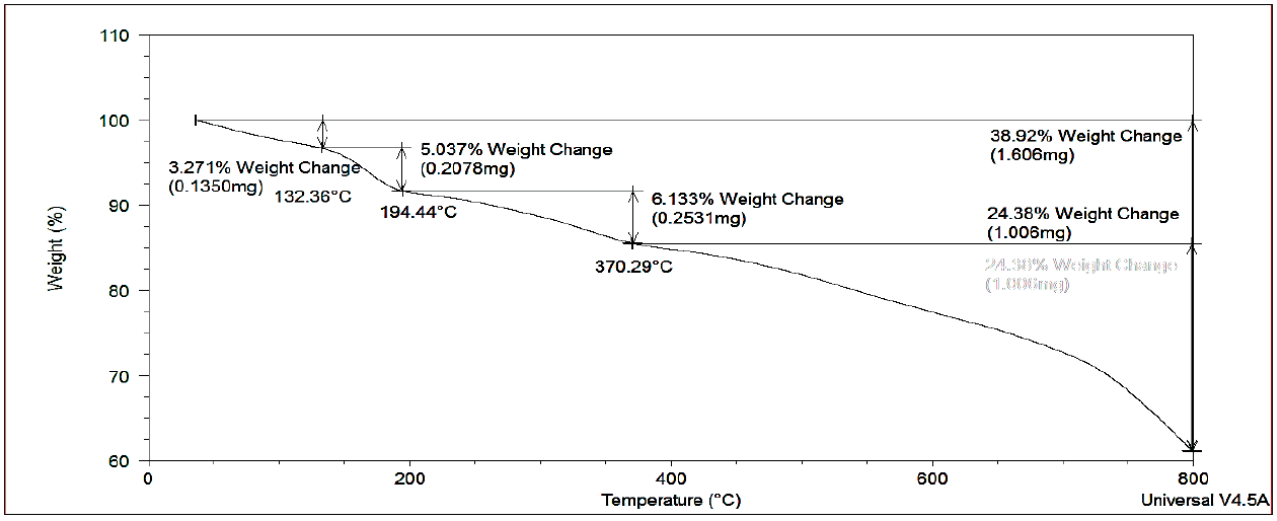

Figure 6. TGA of [Co(HL)Cl_2 H_2O] analyses in N_2 atmosphere conditions.

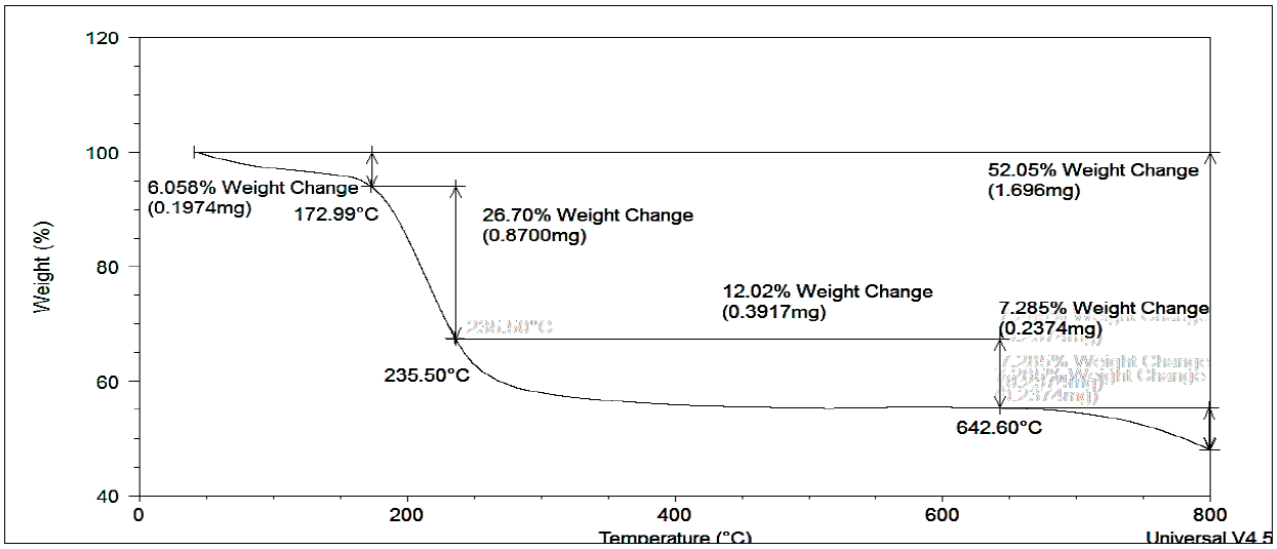

Figure 7. TGA of $[Cu(HL)Cl_2 H_2O]$ in N_2 atmosphere.

the ring. Zn(II)-complex almost had the highest antibacterial activity compared to other compounds. This is because, in comparison to those of other metal complexes, both their molecular weight and electronic configuration (using the d10 system) are on the lighter side. Compared to the free bonds and the other complexes, the cadmium (II) complex demonstrated significantly higher activity levels against all of the bacterial strains. As a result, we are now in a position to discuss the activity of the complexes in light of the chelation theory and the Overton model[28]. It describes the capacity of the metal component to penetrate the bacterial cell layer. The positive charge on the metal core will then be reduced due to this process, ultimately leading to coordinated bonding between the N and O atoms. Because of this, the lipophilic nature of the metal chelate system will increase, facilitating its movement across the lipid layer in the cell membranes of microorganisms. The research on the antifungal properties of semicarbazone ligand (HL) and its derivatives was conducted using two distinct kinds of fungi as test subjects (Candida and Rhizosporium), Table No. 5, which shows that the association found evidence of activity against both types of fungi. Compared to free ligands, HL complexes demonstrated much higher levels of antibacterial activity against all species of bacteria (HL). It was discovered that the molecule with the formula Cd(II) is more potent against (Candida and Rhizosporium). Because of the research that has been presented up until this point, new tridentate Schiff-base ligands have been tested to determine whether they are effective against a wide variety of pathogenic bacteria, viruses, and parasites. As mentioned earlier, the analysis was carried out to determine the effectiveness of these ligands. Some of these bacteria include *Clostridium perfringens*[29], *Brucella melitensis*[30], *Proteus vulgaris*[31,32], *Staphylococcus aureus*[33], *Pseudomonas aeruginosa*[34], and *Toxoplasma spp*[35,36], SARS-Cov-2[37]

Conclusions

The present study synthesized and described a carbazone half-ligand (HL) and its metal complexes. In monomer isolation, this is formed when the ligand combines with Mn(II), Co(II), Ni(II), Cu(II), Zn(II), and Cd(II) metal ions in a 1:1 (L: M) mol ratio. Physical, chemical, and spectroscopic investigations illuminated complex structures and linkages. These results yield compounds with quaternary or hexagonal coordination. The effectiveness of the ligand and its derivatives against bacteria and fungus was investigated. Free ligands were more bactericidal than semicarbazone complexes.

Funding

Self-Funding.

Conflicts of Interest

The authors declare no conflict of interest.

Compounds	*Escherichia coli* (G−)	*Pseudomonas aeruginosa*(G−)	*Bacillus stubtilis* (G+)	*Staphylococcus aureus* (G+)	*Candida*	*Rhizopus porium*
HL	13	14	13	12	17	**15**
$[Mn(HL)_2Cl_2]$	18	12	15	20	21	**20**
$[Co(HL)_2Cl_2].H_2O$	20	20	20	21	22	**25**
$[Ni (HL)_2 Cl_2]$.	16	15	17	16	20	**16**
$[Cu(HL)_2Cl_2].H_2O$	19	17	16	13	20	**15**
$[Zn (HL)_2].Cl_2$	16	15	17	16	19	**16**
$[Cd (HL)_2].Cl_2$	**22**	**26**	**22**	**21**	**23**	**30**

Table 5. The inhibition zones (mm) of antibacterial activity and antifungal activity for ligand and their complexes.

Bibliographic references

1. Cotton FA, Wilkinson G, Murillo CA, Bochmann M. Advanced inorganic chemistry. John Wiley and Sons, Inc.; 1999.
2. Hadi Kadhim S, Abd-Alla Q. I, Jawad Hashim T. Synthesis and Characteristic Study of Co (II), Ni (II) And Cu (II) Complexes of New Schiff Base Derived from 4-Amino Antipyrine. Int J Chem Sci. 2017; 15(1):107.
3. Hathaway BJ, Wilkinson G, Gillard RD, McCleverty JA. Comprehensive coordination chemistry. The synthesis, reactions, properties and applications of coordination compounds. 1987; 5 (1):533-774.
4. Sathe BS, Jayachandran E, Jagtap VA, Sreenivasa GM. Synthesis and antibacterial, antifungal activity of novel analogs of fluoro benzothiazole Schiff's base. Journal of Chemical and Pharmaceutical Sciences. 2010; 3(4):216-217.
5. Sondhi SM, Singh N, Kumar A, Lozach O, Meijer L. Synthesis, anti-inflammatory, analgesic and kinase (CDK-1, CDK-5 and GSK-3) inhibition activity evaluation of benzimidazole/benzoxazole derivatives and some Schiff's bases. Bioorganic & medicinal chemistry. 2006;14(11):3758-3765.
6. Sondhi SM., Singh N, Kumar A, Lozach O, Meijer L. Synthesis, anti-inflammatory, analgesic and kinase (CDK-1, CDK-5 and GSK-3) inhibition activity evaluation of benzimidazole/benzoxazole derivatives and some Schiff's bases. Bioorganic & medicinal chemistry, 2006; 14(11):3758-3765.
7. Chaubey AK, Pandeya SN. Synthesis & anticonvulsant activity (Chemo Shock) of Schiff and Mannich bases of Isatin derivatives with 2-Amino pyridine (mechanism of action). International Journal of PharmTech Research. 2012;4(4):590-598.
8. Aboul-Fadl T, Mohammed FA, Hassan EA. Synthesis, antitubercular activity and pharmacokinetic studies of some Schiff bases derived from 1-alkylisatin and isonicotinic acid hydrazide (INH). Archives of pharmacal research. 2003;26(10):778-784.
9. Wei D, Li N, Lu G, Yao K. Synthesis, catalytic and biological activity of novel dinuclear copper complex with Schiff base. Science in China Series B. 2006;49(3):225-229.
10. Avaji PG, Kumar CV, Patil SA, Shivananda KN, Nagaraju C. Synthesis, spectral characterization, in-vitro microbiological evaluation and cytotoxic activities of novel macrocyclic bis hydrazone. European Journal of medicinal chemistry. 2009;44(9):3552-3559.
11. Samraa Ali Hussein and Enaam Ismail Yousif. Metal complexes of semicarbazone ligand derived from Mannich-β-aminocarbonyl : Synthesis, structural characterisation, thermal properties and biological activity. Biochem. Cell. Arch. 2021; 21(2): 4855-4863. DocID: https://connectjournals.com/03896.2021.21.4855.
12. Yousif EI, Hussien AK, Hasan HA.COII, NIII and CDII complexes derived from mixed Azo-linked schift base ligands: Formation, characterization, thermal analysis and biological study. Plant Archives, 2020; 20(1):2405-2411.
13. Ahmed AI, Yousif EI. New Metal Complexes with AZO ligand; Synthesis, Spectral Characterisation and Biological Evaluation. Pakistan Journal of Medical & Health Sciences. 2022; 16(07):550-554.
14. Gow NA, Van De Veerdonk FL, Brown AJ, Netea MG. Candida albicans morphogenesis and host defence: discriminating invasion from colonization. Nature reviews microbiology. 2012; 10(2):112-122.
15. Hussain SA, Al-Jeboori MJ. New metal complexes derived from Mannich-base ligand; Synthesis, spectral characterisation and biological activity. J. Global Pharma Tech. 2019; 11(2):548-560.
16. Nakamoto, K. Infrared Spectra of Inorganic and Coordination Compounds. John Wiley and Sons, New York, 1996. 4th Edn.
17. Volkert WA, Hoffman TJ. Therapeutic radiopharmaceuticals. Chemical reviews. 1999;99(9):2269-2292.
18. Bal S, Bal SS. Cobalt (II) and Manganese (II) complexes of novel Schiff bases, synthesis, charcterization and thermal, antimicrobial, electronic, and catalytic features. Adv. Chem. 2014;2014:1-2.
19. Castonguay LA, Treasurywala AM, Caulfield TJ, Jaeger EP, Kellar KE. Prediction of q-values and conformations of gadolinium chelates for magnetic resonance imaging. Bioconjugate chemistry. 1999; 10(6):958-964.
20. Hasan HA, Yousif EI, Al-Jeboori MJ. Metal-assisted assembly of dinuclear metal (II) dithiocarbamate Schiff-base macrocyclic complexes: Synthesis and biological studies. Global J. Inorg. Chem. 2012; 3(10):1-7.
21. Abass RU, Yousif EI. New Metal Complexes Derived from Schiff-Base Ligand: Synthesis Structural Characterisation, Thermal Properties and Biological Evaluation. HIV Nursing. 2022; 22(2):3561-3571.
22. Ramachandran E, Gandin V, Bertani R, Sgarbossa P, Natarajan K, Bhuvanesh NS, Venzo A, Zoleo A, Glisenti A, Dolmella A, Albinati A. Synthesis, characterization and cytotoxic activity of novel copper (II) complexes with aroylhydrazone derivatives of 2-Oxo-1, 2-dihydrobenzo [h] quinoline-3-carbaldehyde. Journal of Inorganic Biochemistry. 2018; 182:18-28.
23. Dong XY, Kang QP, Li XY, Ma JC, Dong WK. structurally characterized solvent-induced homotrinuclear cobalt (II) N2O2-donor bisoxime-type complexes. Crystals. 2018; 8(3):139-141.
24. Hassaan AM, Khalifa MA, Shehata AK. COMPLEXES OF SOME METAL IONS WITH A SCHIFF BASE LIGAND DERIVED FROM ISATIN AND O□AMINOPHENOL. Bulletin des Sociétés Chimiques Belges. 1995; 104(3):121-124.
25. Souza P, Mendiola MA, Matesanz AI, Fernández V, Arquero A. Synthetic and physicochemical studies of divalent metal complexes with cyclic hydrazone and semicarbazone ligands. Transition Metal Chemistry. 1995; 20(2):157-161.
26. Lever, A. B. P. Inorganic Electronic Spectroscopy, Elsevier Publishing House, Amsterdam-London-New York. 1984.
27. Choudhary MI, Thomsen WJ. Bioassay techniques for drug development. CRC Press; 2001.
28. Singh RV, Dwivedi R, Joshi SC. Synthetic, magnetic, spectral, antimicrobial and antifertility studies of dioxomolybdenum (VI) unsymmetrical imine complexes having a No N donor system. Transition Metal Chemistry. 2004;29(1):70-74.
29. Hashim ST, Fakhry SS, Rasoul LM, Saleh TH, Alrubaii BA. Genotyping toxins of Clostridium perfringens strains of rabbit and other animal origins. Tropical Journal of Natural Product Researchthis link is disabled. 2021;5(4):613-616.
30. abdulkaliq Awadh H, Hammed ZN, Hamzah SS, Saleh TH, AL-Rubaii BA. Molecular identification of intracellular survival related Brucella melitensis virulence factors. Biomedicine. 2022;42(4):761-765.
31. Abdul-Gani MN, Laftaah BA. Purification and characterization of chondroitinase ABC from Proteus vulgaris, an Iraqi clinically isolate. Current Science. 2017:2134-2140.
32. kadhim AL-Imam MJ, AL-Rubaii BA. The influence of some amino acids, vitamins and anti-inflammatory drugs on activity of chondroitinase produced by Proteus vulgaris caused urinary tract infection. Iraqi Journal of Science. 2016:2412-2421.
33. Sabah Fakhry S, Noori Hammed Z, Abdul-elah Bakir W, Abdullah Laftaah ALRubaii B. Identification of methicillin-resistant strains of Staphylococcus aureus isolated from humans and food sources by Use of mecA 1 and mecA 2 genes in Pulsed-field gel electrophoresis (PFGE (technique. Revis Bionatura 2022; 7 (2) 44. http://dx.doi.org/10.21931/RB/2022.07.02.44.
34. Shehab ZH, AL-Rubaii BA. Effect of D-mannose on gene expression of neuraminidase produced from different clinical isolates of Pseudomonas aeruginosa. Baghdad Science Journal. 2019;16(2):291–298.
35. Abdulla L, Ismael MK, Salih TA, Malik SN, Al-Rubaii BA. Genotyping and evaluation of interleukin-10 and soluble HLA-G in abortion due to toxoplasmosis and HSV-2 infections. Annals of parasitology. 2022;68(2):385-390.
36. Jiad AL, Ismael MK, Muhsin SS, Al-Rubaii BA. ND2 Gene Sequencing of Sub fertile Patients Recovered from COVID-19 in Association with Toxoplasmosis. Bionatura. 2022;7(3):45. http://dx.doi.org/10.21931/RB/2022.07.03.45.
37. Rasoul LM, Nsaif MM, Al-Tameemi MT, Al-Rubaii BA. Estimation of primer efficiency in multiplex PCR for detecting SARS-Cov-2 variants. Bionatura, 2022, 7(3), 48. http://dx.doi.org/10.21931/RB/2022.07.03.49.